

## RESEARCH ARTICLE

## Effect of annular solar eclipse on ionospheric total electron content over low latitude

Chaithra P<sup>1,\*</sup> , Kamsali Nagaraja<sup>2</sup> <sup>1</sup>Atmospheric and Space Science Research Laboratory, Department of Physics, Bangalore University, Bengaluru, 560056, India<sup>2</sup>Atmospheric and Space Science Research Laboratory, Department of Physics, Bangalore University, Bengaluru, 560056, India

## Abstract

Solar eclipses provide a distinctive opportunity to study the interactions between solar radiation and the Earth's ionosphere. This study focuses on the ionospheric response, particularly Total Electron Content (TEC) variations, during the annular solar eclipse on December 26, 2019. TEC from four GNSS stations, YIBL (22.186 °N, 56.112 °E), IISC (13.021 °N, 77.570 °E), HYDE (17.417 °N, 78.551 °E), and GUUG (13.433 °N, 144.803 °E) was analyzed using dual-frequency GPS receiver data. During the solar eclipse, TEC decreased at all four stations; the maximum reductions were observed at IISC (33.12%), HYDE (32.01%), GUUG (29.73%), and YIBL (26.33%). To observe the influence of the geomagnetic storm on TEC during the eclipse, the study analyses the Dst index, Kp index, interplanetary magnetic field (Bz), and electric field (Ey). The study showed that storm activity did not influence TEC during the solar eclipse and that the observed change in TEC was due solely to the eclipse on December 26, 2019. The study compares IRI-2020 model TEC data and observed TEC data during storm days. The results also showed a good correlation between them at IISC, HYDE, and GUUG, whereas there was a moderate correlation at YIBL. The findings provide essential understanding of ionospheric behaviour during eclipses and elucidate the need to improve ionospheric models with real events to improve space weather forecasting and reliability of satellite communications.

**Keywords:** Solar eclipse, ionosphere, TEC, geomagnetic storm, disturbed storm time

**Cite this article as:** Chaithra, P., & Nagaraja, K. (2026). Effect of annular solar eclipse on ionospheric total electron content over low latitude. *Journal of Thermal Engineering*, 12(4), 1359–1367. <https://doi.org/10.47481/jten.0035>

## 1. Introduction

The ionosphere is a major layer of the upper atmosphere that undergoes some dynamic changes during these events as well as the Total Electron Content (TEC) [1, 2]. The ionospheric Total Electron Content (TEC) is measured by the number of free electrons along a path through the ionosphere and is an important parameter in the study of ionospheric density and its variability [3, 4]. TEC is also sensitive to the solar radiation and this affects the ion production directly by photoionization [5]. During a solar eclipse, the temporary obstruction of solar radiation by the Moon significantly reduces photoionization in the ionosphere. Since ionospheric plasma is primarily sustained by solar ultraviolet and extreme ultraviolet radiation, a sudden decrease in solar radiation reduces the production of free electrons and thus decreases TEC. Solar eclipses cause changes in the incoming solar radiation to the ionosphere, resulting in modifications to the ionization and electron density

of the ionosphere [6]. The partial obstruction or total obstruction of the moon to the incoming solar radiation causes a temporary reduction in ionospheric electron density known as a solar eclipse [7, 8]. Many researchers have studied the effect of different solar eclipses on the ionosphere TEC measurements [9-12]. Solar eclipses provide a unique natural laboratory for studying transient changes in ionospheric TEC, because they cast a temporary shadow that modulates the solar radiation reaching the ionosphere. Sudden fall in ionization during an eclipse with a rapid recovery provides information about the dynamics of ionospheric reaction to rapid variations in solar flux [13].

Annular solar eclipses, where the moon covers the sun's center, leaving a ring-like appearance, have been observed to cause significant changes in the ionospheric TEC [14]. Several studies have examined the ionospheric TEC fluctuation during December 26, 2019 annular solar eclipse [14-19]. Senapathi et

\*Corresponding Author

E-mail Address: chaithra.assrphy7@gmail.com

Submitted: 7 February 2025 ; Accepted: 31 May 2025

This paper was recommended for publication in revised form by Editor-in-Chief Ahmet Selim Dalkılıç



al., (2020) investigated the spatiotemporal variations in ionospheric TEC over the Southeast Asian region during the solar eclipse on December 26, 2019. The simulations using their SAMI3 model closely resembled real TEC variations and showed significant TEC depletion. Surprisingly, they also observed that the eclipse caused ionosphere dynamics that led to high TEC in both northern Japan and the adjacent Pacific Ocean [15]. The article by Shagimuratov et al., (2021) explored the TEC response towards the annular solar eclipse on June 21, 2020, using GPS observations. They analysed the results and found that a TEC depression had reached a minimum around the eclipse maximum, and this demonstrates that the ionospheric behaviour is uniform during periods of eclipses [14]. By conducting multi-instrument observations in India and South Asia, Barad et al., (2022) studied how the ionosphere responded to the solar eclipse on December 26, 2019. Their findings proved the complicated character of the ionospheric disturbances such events cause since they showed a strong sporadic E-layer formation throughout the eclipse and pointed out a 30-40% drop in TEC [16]. In the same eclipse, Harjosuwito et al., (2023) studied the time changes in TEC across Indonesia, revealing that the percentage changes in foF2 in Kotabang and Pontianak were 24.0% and 27.5% reduced, respectively. This analysis revealed electrodynamic mechanisms manipulated by the ionosphere reactions to solar eclipses [17]. Choudhary et al., (2024) investigated the effects of equatorial Indian pre-noon annular solar eclipses. Based on their study, the ionospheric F-layer exhibited some upward and downward motions following the eclipse implying that there were complicated vertical plasma motions, and the Equatorial Electrojet (EEJ) was weakened during and after the eclipse [18]. In the eclipse of December 26, 2019 Khamdan et al., (2024) identified variation in ionospheric TEC in various GNSS stations in Asia. They noted that recombination and photochemical processes influenced time delays in TEC response, and they found a 30% depletion of TEC in most of the stations [19].

The ionosphere undergoes complex dynamics related to reduced photoionization, recombination, and possible wave-like chains arising from rapid variations in solar illumination. The temporary shadowing effect has effects on the F-region electron density with TEC reductions highest just after the eclipse maximum [20]. These effects are also influenced by local geomagnetic conditions and pre-existing ionospheric structures, such as the equatorial anomaly. Multiple studies have investigated the ionospheric response to solar eclipses using both observational data and models such as the International Reference Ionosphere (IRI). Lin et al., (2012) compared observed TEC with IRI-2007 and discovered that the MAGIC model performed better with observations during the eclipse on July 22, 2009, while the IRI model was unable to effectively reproduce eclipse-induced TEC depletion [21]. Atıcı et al., (2021) investigated ionospheric electron density variations during partial solar eclipses on March 29, 2006, and March 20, 2015, and compared the results to IRI-2016 forecasts, showing inconsistencies between modelled and observed values [22].

Nevertheless, a multi-station analysis across low-latitude regions is still needed relative to previous research, particularly one that directly compares actual TEC variations with forecasts from the IRI-2020 model. This research seeks to contribute to the body of knowledge on ionospheric dynamics during an eclipse at equatorial latitudes. The present experiment examines changes in TEC during the solar eclipse of 26 December 2019. It is anticipated that the findings will improve TEC model predictions during sudden changes in solar flux, thereby improving space weather forecasting. This will enhance the reliability of GNSS-based navigation, positioning, and satellite communication systems in the event of a similar solar eclipse.

## 2. Data and methodology

TEC variations can be studied in many ways, and one of them is the Global Navigation Satellite System (GNSS) network, which provides dynamics of the Earth's ionosphere coupled process [23]. The study uses the TEC data from the International GNSS network stations YIBL (22.186 °N, 56.112 °E), IISC (13.021 °N, 77.570 °E), HYDE (17.417 °N, 78.551 °E), and GUUG (13.433 °N, 144.803 °E), whose locations are shown in Figure 1. The four GNSS stations were selected for their geographic locations to provide representative coverage of the low-latitude ionosphere, focusing on regions influenced by the Equatorial Ionization Anomaly (EIA) and by varying eclipse obscuration rates. Table 1 provides the GNSS stations used in the study, the eclipse duration, and the obscuration rate. The eclipse's influence extends beyond its path to nearby locations. Therefore, it is important to examine the spatial distribution of these effects. Figure 2 shows the path of the annular solar eclipse that occurred on December 26, 2019. When points P1 and P4 are in external contact with the penumbra, points P3 and P4 are in internal contact with the penumbra. The external part of the penumbral time of contact refers to the beginning of the eclipse, which occurred at 02:29:43.5 UT (P1), and its end, at 08:05:36.1 UT (P4), on December 26, 2019. The total duration of the greatest eclipse is 03 min 39.5 sec. The width of the eclipse path is 119.9 km. The magnitude of the eclipse is 0.9701.

The ionospheric TEC data are obtained from CDDIS, which is in Rinex format [24]. Ionospheric TEC is estimated from dual-frequency GNSS measurements using the GPS-TEC software developed by Gopi Seemala. It uses the RINEX observation and navigation files to compute slant TEC from L1 and L2 signals. The software then assumes a thin-shell model of the ionosphere and uses a mapping function to convert Slant TEC to Vertical TEC. Additionally, it applies modifications from international GNSS stations for receiver and satellite differential code biases [25]. This software helps to obtain Vertical Total Electron Content (VTEC), which is measured in TECU, where one TECU =  $10^{16}$  electrons/m<sup>2</sup> [26]. Geomagnetic data such as the Disturbed storm time (Dst) index is obtained from Kyoto webserver [27], Planetary-K (Kp) index, Interplanetary Magnetic field (IMF-Bz), and Interplanetary Electric field (IEF-Ey) are obtained from the Omniweb data explorer. The Observed TEC data were compared with the IRI-2020 model data during the annular solar eclipse on December 26, 2019. The IRI-2020 model is an update

to the previous version, IRI-2016. It improves accuracy and provides a deeper understanding of the ionosphere by including more recent data and updated algorithms. Table 2 lists the parameters used in the study and their data sources. The percentage change in VTEC is

calculated using the following relation. This equation quantifies the relative change in VTEC between the eclipse day and a control (non-eclipse) day, following the approach used in previous studies [13]:

$$\text{Change in VTEC } (\Delta \text{VTEC})\% = \frac{\text{Eclipse day VTEC} - \text{Noneclipse day VTEC}}{\text{Noneclipse day VTEC}} \times 100$$

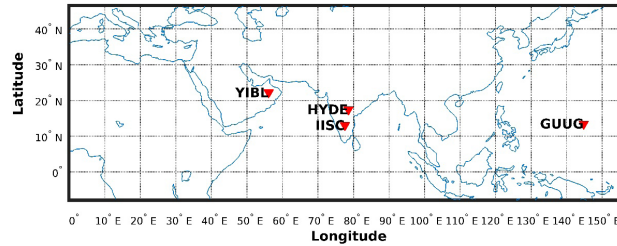


Figure 1. Geographical locations of the GNSS receiver

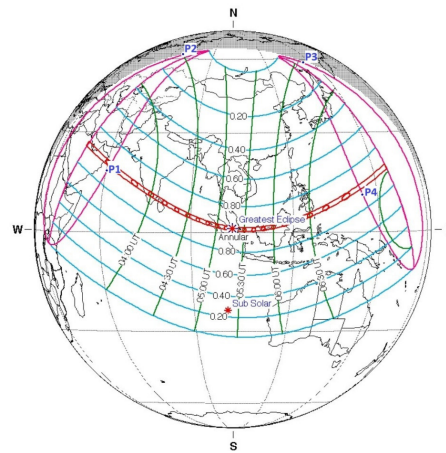


Figure 2. Path of the annular solar eclipse that occurred on December 26, 2019

Table 1. List of GNSS stations and duration of solar eclipse over each station

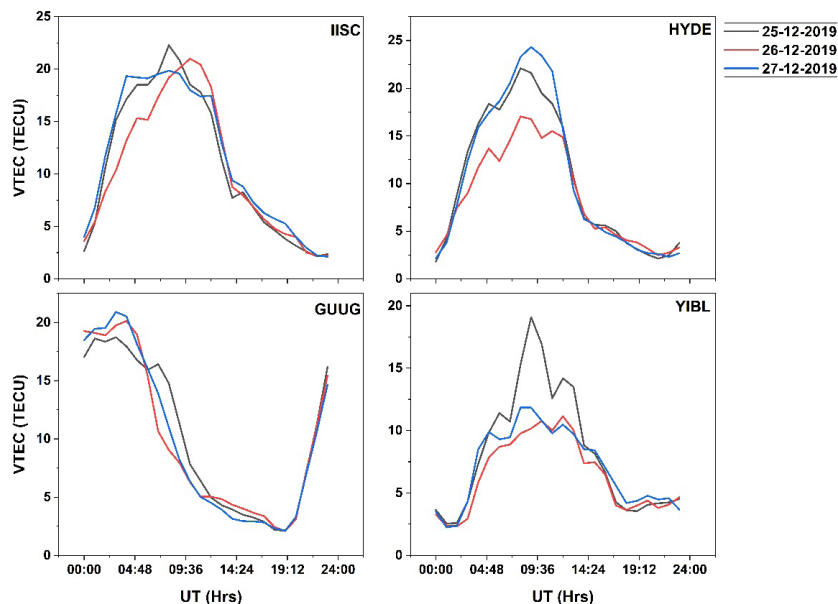
Station code	Geographic latitude	Geographic longitude	Start of eclipse (UT)	Maximum	End of eclipse (UT)	Obscuration rate
YIBL	22.186 °N	56.112 °E	02:30:34.1	03:37:27.8	04:55:06.9	91.90%
IISC	13.021 °N	77.570 °E	02:36:30.0	04:00:00.6	05:41:49.9	89.02%
HYDE	17.417 °N	78.551 °E	02:38:06.5	04:00:40.1	05:40:35.1	73.94%
GUUG	13.433 °N	144.803 °E	05:33:41.9	06:56:02.1	08:05:25.4	91.89%

Table 2. Data source for the parameters used in the present study

Parameters	Data source
Solar Eclipse path	<a href="https://eclipse.gsfc.nasa.gov/">https://eclipse.gsfc.nasa.gov/</a>
Ionospheric TEC	<a href="https://cddis.nasa.gov/">https://cddis.nasa.gov/</a>
Dst index	<a href="https://wdc.kugi.kyoto-u.ac.jp/wdc/Sec3.html">https://wdc.kugi.kyoto-u.ac.jp/wdc/Sec3.html</a>
Kp, IMF-Bz, IEF-Ey	<a href="https://omniweb.gsfc.nasa.gov/form/dx1.html">https://omniweb.gsfc.nasa.gov/form/dx1.html</a>
IRI-TEC	<a href="https://kauai.ccmc.gsfc.nasa.gov/instantrun/iri/">https://kauai.ccmc.gsfc.nasa.gov/instantrun/iri/</a>

### 3. Results and discussion

Figure 3 shows the ionospheric TEC variations at the stations IISC, HYDE, GUUG, and YIBL. The study uses VTEC data from December 25-27, 2019. Here, 25 and 27 December 2019 refers to non-eclipse days, whereas December 26, 2019, refers to the eclipse day. The eclipse over IISC begins at 02:36:30.0 UT, ends at 05:41:49.9 UT, and its rate of obscuration is 89.02%. During the eclipse period, VTEC decreases by 5.109 TECU compared to non-eclipse day over IISC. The eclipse at HYDE begins at 02:38:06.5 UT, ends at 5:40:35.1 UT, and has an obscuration rate of 73.94%. During the eclipse period, VTEC decreased by 5.82 TECU compared to non-eclipse days over HYDE. The beginning of the eclipse over GUUG is 05:33:41.9 UT, the end of the eclipse is 08:05:25.4 UT and the rate of obscuration is 91.89%. During the eclipse period, VTEC decreased by 4.505 TECU compared with non-eclipse days at GUUG. The beginning of the eclipse over YIBL is 02:30:34.1 UT, the end of the eclipse is 04:55:06.9 UT and the rate of obscuration is 91.90%. During the eclipse period, VTEC decreased by 5.109 TECU compared to non-eclipse days over YIBL. Observations show that VTEC decreases during eclipse hours and, after the end of those hours, enters a recovery phase.



**Figure 3.** VTEC variations over IISC, HYDE, GUUG, and YIBL during December 25 - 27, 2019. Time is given in Universal Time (UT) hours, and VTEC values are expressed in TEC Units (TECU)

Figure 5 shows Dst, Kp, and interplanetary electric and magnetic field variations from 25 to 27 December 2019. The shaded area represents the duration of the solar eclipse. The literature shows that the occurrence of the geomagnetic storm will be noticed if the Dst index is less than -30 nT [28]. It was observed that the Dst index did not reach the threshold level of a geomagnetic storm, confirming that no geomagnetic storm occurred during the annular solar eclipse; this is also supported by the interplanetary magnetic field (Bz) varying

Precise observations are made by finding the deviation in VTEC ( $\Delta$ VTEC) during eclipse hours as shown in figure 4. A clear dip in  $\Delta$ VTEC at all four stations was observed during the Moon's umbral shadow on Earth. The percentage decrease in VTEC over IISC is 33.12%, HYDE is 32.01%, GUUG is 29.73% and YIBL is 26.33%. The smaller decrease in TEC at YIBL compared to other stations can be attributed to its geographic location and to the weaker influence of the Equatorial Ionization Anomaly (EIA). Other studies revealed in the previous research have found that the fountain effect influences the instability of TEC over solar eclipses significantly, particularly in the region of the EIA crest [18]. YIBL is further along the magnetic equator; hence, the ionospheric reaction to the eclipse is weaker compared to those farther along, near the EIA. Similar results were found by Barad et al., (2022), who also described large TEC-reductions in spots that were highly affected by the dynamics of the EIA and smaller in magnitude in an area outside the anomaly [16]. Harjosuwito et al., (2023) have also highlighted the relevance of recombination mechanisms in limiting TEC depletion. They observed that recombination and photochemical effects greatly influence TEC changes during eclipses, which may explain why TEC depletion at YIBL was not as intense [17].

from -4 to 6 nT, the interplanetary electric field ( $E_y$ ) varying from -2 to 2 mV/m, and a maximum Kp index of 2. This confirms that changes in ionospheric TEC are mainly attributable to the annular solar eclipse that occurred on December 26, 2019.

The study analyzes the correlation between observed and IRI 2020 model VTEC data, as shown in Figure 6. The correlation coefficient ( $R^2$ ) between observed and modelled VTEC was calculated using

Pearson's correlation method, based on a linear regression analysis. The coefficients of determination ( $R^2$ ) and the associated p-values were computed for four GNSS stations to evaluate the agreement between the observed VTEC and the IRI-2020 model during the annular solar eclipse. The observed and modeled TEC showed significant agreement, with very strong correlations at IISC ( $R^2 = 0.93$ ,  $p = 7.09 \times 10^{-14}$ ) and GUUG ( $R^2 = 0.96$ ,  $p = 3.15 \times 10^{-17}$ ). A strong and statistically significant relationship was observed at HYDE ( $R^2 = 0.81$ ,  $p = 2.24 \times 10^{-9}$ ). At the YIBL station, the correlation between the observed and modeled TEC was moderate, with an  $R^2$  value of 0.60 and a statistically significant p-value of  $8.20 \times 10^{-6}$ . The lower level of agreement may be due to regional ionospheric characteristics or to the model's limited performance over YIBL during the eclipse period. However, the significance of the p-value confirms that the correlation is meaningful and not a result of random variation. Such

correlations support the viability of the IRI 2020 model in predicting changes in VTEC throughout the eclipse. The correlation analysis of IISC, HYDE, and GUUG indicates that the IRI-2020 model is useful for describing the impact of the eclipse on ionospheric changes in these areas. This finding differs from earlier versions of the model, such as the IRI-2007 and IRI-2016 models, which were shown to underrepresent the ionospheric changes associated with eclipses in the earlier studies [21, 22]. Unlike earlier research, which found that electron density and TEC profiles showed significant differences, especially during and after eclipse maxima, current data indicate that IRI2020 provides more consistent predictions of eclipse impacts. Recent findings using IRI-2020 show that the model has become substantially more effective at describing TEC variations during solar eclipses.

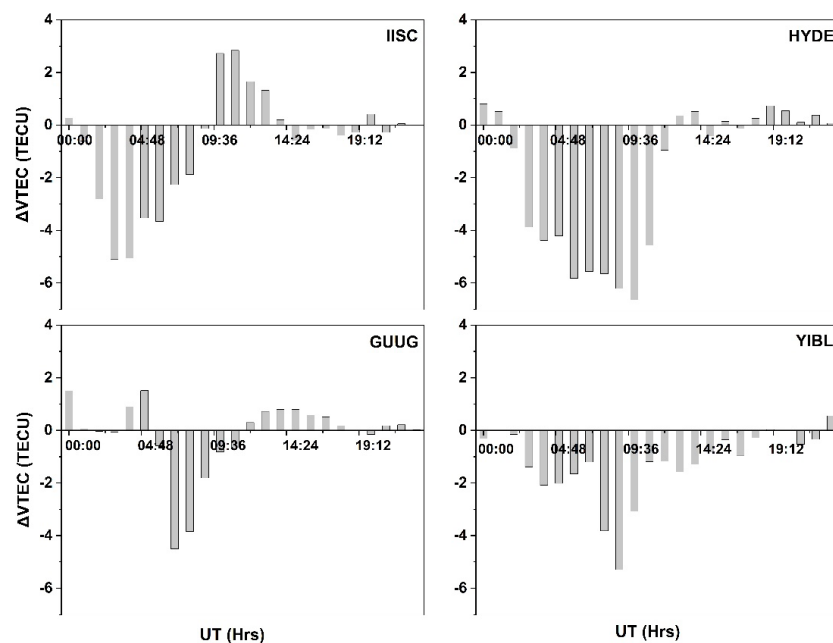


**Figure 4.** Changes in VTEC( $\Delta$ VTEC) over IISC, HYDE, GUUG, and YIBL on the day of the annular solar eclipse (December 26, 2019). Time is shown in Universal Time (UT) hours, and  $\Delta$ VTEC is in TEC Units (TECU)

The moderate correlation at YIBL ( $R^2=0.60$ ) may not just be due to its geomagnetic position being outside the EIA area, but also due to other geophysical and electrodynamic factors. These might include local electrodynamic-drift, neutral-wind, and ionospheric-composition variations that are not adequately represented by empirical models such as IRI-2020. The IRI-2020 model is based on the average of the climatology without fully explaining short-term variations due to local electrodynamic processes [29]. The YIBL results suggest that additional modification may still be necessary for some locations, although this finding confirms the applicability of the IRI-2020 model to equatorial and low-latitude regions. A comparative presentation across four stations reveals varying VTEC reactions to the eclipse. Both the IISC and HYDE stations, located on the EIA crest, exhibited the largest percentage changes in VTEC

(33.12% and 32.01%, respectively), indicating a strong effect of EIA dynamics during the period of solar obstruction. GUUG, an international station, is also located close to the EIA area and has revealed a significant decrease in VTEC of 29.73%, which is consistent with its high rate of obscuration (91.89%). Conversely, YIBL, which is not within the main range of influence of the EIA, had the smallest VTEC reduction (26.33%) and weakest correlation ( $R^2 = 0.60$ ) with the IRI-2020 model, suggesting more complicated local electrodynamic behaviour. This comparison across stations highlights the importance of latitude and regional ionospheric processes in moderating changes in TEC during eclipses.

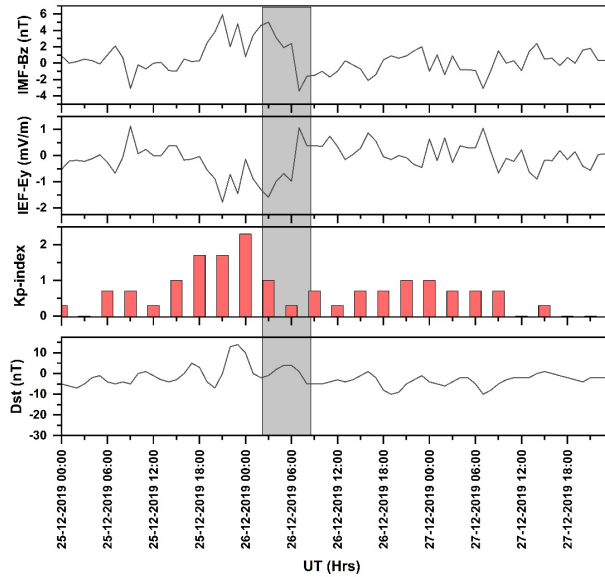


**Figure 5.** Variation of Disturbed storm time (Dst), Planetary K (Kp) index, Interplanetary Electric field (Ey), and Interplanetary magnetic field (Bz) during December 25-27, 2019

Other latitude-related factors, such as geomagnetic latitude, background ionospheric conditions, and local electrodynamic processes, can also contribute to the variations in eclipse impact observed among stations, in addition to proximity to the Equatorial Ionization Anomaly (EIA). The EIA remains dominant in the low-latitude ionosphere. Our results have significant implications for GNSS-based navigation and satellite communications systems, which require proper ionospheric delay modeling. Knowledge of TEC dynamics during solar eclipses, which lead to rapid and localized ionospheric

perturbations, enhances the reliability of GNSS signals and the accuracy of space weather prediction tools. This would be critical for aviation, maritime navigation, and emergency response systems that require satellite positioning. Further studies are necessary, including localized electrodynamic studies and coordinated observations (ground-based radars, magnetometers, and GNSS networks). The use of real-time GNSS TEC measurements in adaptive ionospheric models will facilitate improved and timely forecasts of dynamic ionospheric variations, such as solar eclipses and geomagnetic storms.

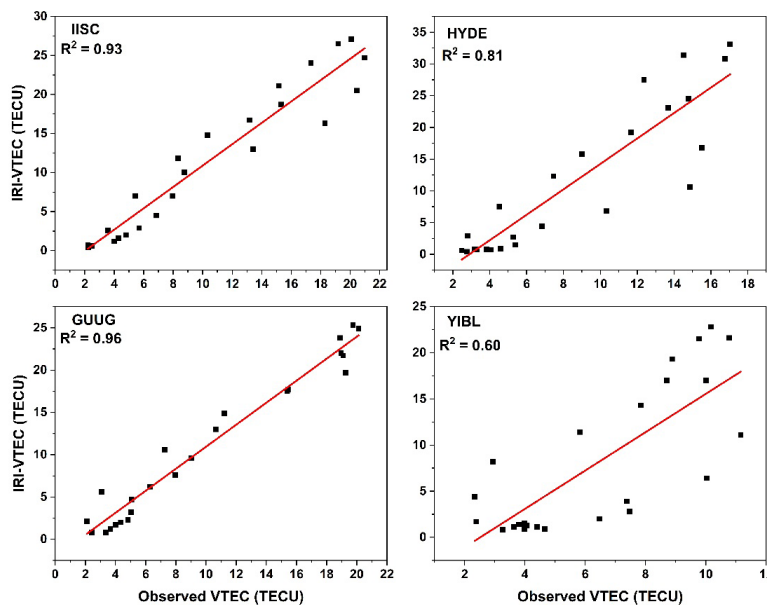


**Figure 6.** Correlation between IRI-2020 model VTEC and observed VTEC during December 26, 2019, solar eclipse

#### 4. Conclusion

With reference to the analysis of the ionospheric TEC variations observed at the stations IISC, HYDE, GUUG, and YIBL, the study reports important findings regarding the annular solar eclipse that occurred on December 26, 2019. The findings show a notable decrease in VTEC during the eclipse hours and in the post-eclipse period. The level of obscuration and the degree of VTEC decrease also differed among the various stations, with IISC and GUUG recording the highest obscuration rates of 89.02 and 91.89, respectively. The study reports significant reductions in VTEC: IISC by 33.12, HYDE by 32.01, GUUG by 29.73, and YIBL by 26.33. The TEC depletion was most observed in the case of IISC and HYDE, which indicated that the effect of the eclipse was not effective in the areas that were heavily affected due to the Equatorial Ionization Anomaly (EIA). The minor decrease in VTEC at YIBL can be explained by its geomagnetic latitude, relatively lower EIA impact, and possible recombination processes.

The research also confirms that no geomagnetic storms occurred during the eclipse, as indicated by the Dst and Kp indices and by variations in the interplanetary magnetic field. The study also indicates that the ionospheric TEC variations observed during the annular solar eclipse on December 26, 2019, were mainly due to the eclipse. A crucial contribution of this work is the comparison of observed VTEC values to those anticipated by the IRI-2020 model. The analysis shows strong correlations ( $R^2 = 0.93, 0.81, \text{ and } 0.96$  of IISC, HYDE, and GUUG, respectively) and demonstrates that the IRI-2020 model significantly outperformed earlier visions in simulating ionospheric responses induced by eclipses. The moderate relationship at YIBL ( $R^2$  of 0.60) demonstrates the restriction of the model on localized and short-term trends at other outside EIA regions. The results serve as valuable data to enhance ionospheric modelling in the future, particularly to forecast the temporary weather features in space, such as the solar eclipses. This research provides the basis for creating a more predictable tool to increase confidence in satellite-based positioning, navigation, and communication systems by improving understanding of TEC variations at a more localized scale. Science and everyday life also require investigation on the short-timescale ionosphere and real-time data synthesis to enhance global models, which are required in regional model changes. The findings have not only offered additional scientific insights into the behaviour of the ionosphere during solar eclipses but have also been of practical relevance by supporting better TEC forecasting models. These inventions can be effective in enhancing navigation, positioning, and confidence in satellite communications when there are sudden changes in solar flux.

#### Nomenclature

CDDIS	Crustal Dynamics Data Information System
Dst	Disturbed storm time
EEJ	Equatorial Electro Jet
EIA	Equatorial Ionization Anomaly

foF2	Frequency of F2 layer
GNSS	Global Navigation Satellite System
GPS	Global Positioning System
GUUG	Mangilao GNSS station in United States of America
HYDE	Hyderabad GNSS station in India
IEF-Ey	Interplanetary Electric Field
IISC	Indian Institute of Science GNSS station at Bengaluru, India
IMF-Bz	Interplanetary Magnetic Field
IRI	International Reference Ionosphere
Kp index	Planetary K index
MAGIC	Model-based Assimilation of GPS-based Ionospheric data
NASA	National Aeronautics and Space Administration
RINEX	Receiver Independent Exchange Format
SAMI3	Sami3 is seamless, 3-dimensional, physics-based model of ionosphere
TEC	Total Electron Content
TECU	Total Electron Content Unit
UT	Universal Time
VTEC	Vertical Total Electron Content
$\Delta$ VTEC	Deviation in Vertical Total Electron Content
YIBL	Yibal GNSS station in Oman

#### Acknowledgements

The authors are grateful to the Crustal Dynamics Data Information System (CDDIS), which has provided valuable ionospheric data. The Data Analysis Centre of Geomagnetism and Space Magnetism at Kyoto University provided the authors with their invaluable geomagnetic data, and the NASA web server provided the authors with data on the annular solar eclipse.

#### References

- [1] Buonsanto, M.J.: Ionospheric Storms - A Review. *Space Sci Rev.* 88, 563-601(1999). <https://doi.org/10.1023/A:1005107532631>
- [2] Idosa, C., Adhikari, B., Shogile, K.: Features of ionospheric total electron content over high latitude regions during geomagnetic storm of November 04, 2021. *Indian Journal of Physics.* 97, 3745-3757(2023). <https://doi.org/10.1007/s12648-023-02746-4>
- [3] Lean, J.L., Meier, R.R., Picone, J.M., Sassi, F., Emmert, J.T., Richards, P.G.: Ionospheric total electron content: Spatial patterns of variability. *J Geophys Res Space Phys.* 121,(2016). <https://doi.org/10.1002/2016JA023210>
- [4] Nishioka, M., Saito, S., Tao, C., Shiota, D., Tsugawa, T., Ishii, M.: Statistical analysis of ionospheric total electron content (TEC): long-term estimation of extreme TEC in Japan. *Earth, Planets and Space.* 73, 52(2021). <https://doi.org/10.1186/s40623-021-01374-8>
- [5] Golubkov, G. V., Manzhelii, M.I., Karpov, I. V.: Chemical physics of the upper atmosphere. *Russian Journal of Physical Chemistry B.* 5, 406-411(2011). <https://doi.org/10.1134/S1990793111030055>

- [6] Chauhan, V., Vishakha, Singh, R., Singh, S., Singh, V., Singh, O.P.: The dynamic effects of solar eclipses of October 25, 2022, and October 14, 2023, on GPS-derived total electron content. *Geod Geodyn.* 16, 75-86(2025). <https://doi.org/10.1016/j.geog.2024.06.003>
- [7] Ding, F., Wan, W., Ning, B., Liu, L., Le, H., Xu, G., Wang, M., Li, G., Chen, Y., Ren, Z., Xiong, B., Hu, L., Yue, X., Zhao, B., Li, F., Yang, M.: GPS TEC response to the 22 July 2009 total solar eclipse in East Asia. *J Geophys Res Space Phys.* 115, (2010). <https://doi.org/10.1029/2009JA015113>
- [8] He, L., Heki, K., Wu, L.: Three-Dimensional and Trans-Hemispheric changes in Ionospheric Electron Density caused by the great Solar Eclipse in North America on 21 August 2017. *Geophys Res Lett.* 45, (2018). <https://doi.org/10.1029/2018GL080365>
- [9] Tsai, H.F., Liu, J.Y.: Ionospheric total electron content response to solar eclipses. *J Geophys Res Space Phys.* 104, 12657-12668(1999). <https://doi.org/10.1029/1999JA900001>
- [10] Afraimovich, E.L., Palamartchouk, K.S., Perevalova, N.P., Chernukhov, V. V., Lukhnev, A. V., Zalutsky, V.T.: Ionospheric effects of the solar eclipse of March 9, 1997, as deduced from GPS data. *Geophys Res Lett.* 25, 465-468 (1998). <https://doi.org/10.1029/98GL00186>
- [11] Jakowski, N., Stankov, S.M., Wilken, V., Borries, C., Altadill, D., Chum, J., Buresova, D., Boska, J., Sauli, P., Hruska, F., Cander, Lj.R.: Ionospheric behaviour over Europe during the solar eclipse of 3 October 2005. *J Atmos Sol Terr Phys.* 70, 836-853(2008). <https://doi.org/10.1016/j.jastp.2007.02.016>
- [12] Silwal, A., Gautam, S.P., Chapagain, N.P., Karki, M., Poudel, P., Ghimire, B.D., Mishra, R.K., Adhikari, B.: Ionospheric Response over Nepal during the 26 December 2019 Solar Eclipse. *Journal of Nepal Physical Society.* 7, 25-30(2021). <https://doi.org/10.3126/jnphysoc.v7i1.36970>
- [13] Gautam, S.P., Muluye Tilahun, A., Silwal, A., Adhikari, B., Getachew Ejigu, Y.: Ionospheric response to the 08 April 2024 total solar eclipse over United States: a case study. *Astrophys Space Sci.* 369, 108 (2024). <https://doi.org/10.1007/s10509-024-04372-w>
- [14] Shagimuratov, I.I., Zakharenkova, I.E., Tepenitsyna, N.Yu., Yakimova, G.A., Efishov, I.I.: Features of the Ionospheric Total Electronic Content response to the Annular Solar Eclipse of June 21, 2020. *Geomagnetism and Aeronomy.* 61, 756-762(2021). <https://doi.org/10.1134/S001679322105011X>
- [15] Senapati, B., Huba, J.D., Kundu, B., Gahalaut, V.K., Panda, D., Mondal, S.K., Catherine, J.K.: Change in Total Electron Content during the 26 December 2019 Solar Eclipse: Constraints From GNSS Observations and Comparison With SAMI3 Model Results. *J Geophys Res Space Phys.* 125, (2020). <https://doi.org/10.1029/2020JA028230>
- [16] Barad, R.K., Sripathi, S., England, S.L.: Multi-Instrument observations of the Ionospheric response to the 26 December 2019 Solar Eclipse over Indian and Southeast Asian longitudes. *J Geophys Res Space Phys.* 127,(2022). <https://doi.org/10.1029/2022JA030330>
- [17] Harjosuwito, J., Husin, A., Dear, V., Muhamad, J., Faturahman, A., Bahar, A., Syetiawan, A., Pradipta, R.: Ionosonde and GPS total electron content observations during the 26 December 2019 annular solar eclipse over Indonesia. *Ann Geophys.* 41, 147-172(2023). <https://doi.org/10.5194/angeo-41-147-2023>
- [18] Choudhary, R.K., St.-Maurice, J.-P., Ambili, K.M., Tripathi, K.R.: Examining the effects of a pre-noon annular Solar Eclipse on equatorial electrodynamicity: Evidence for a subsequent post-noon enhancement in plasma density. *Advances in Space Research.* 73, 3069-3086(2024). <https://doi.org/10.1016/j.asr.2023.12.047>
- [19] Khamdan, S.S., Musa, T.A., Buhari, S.M., Hozumi, K., Ashcroft, N., Ahmad, N.F., Yatini, C.: Monitoring the ionospheric conditions during the annular solar eclipse December 2019: A case study. *J Atmos Sol Terr Phys.* 260, 106272(2024). <https://doi.org/10.1016/j.jastp.2024.106272>
- [20] Aa, E., Coster, A.J., Zhang, S., Vierinen, J., Erickson, P.J., Goncharenko, L.P., Rideout, W.: 2-D Total Electron Content and 3-D Ionospheric electron density variations during the 14 October 2023 annular Solar Eclipse. *J Geophys Res Space Phys.* 129,(2024). <https://doi.org/10.1029/2024JA032447>
- [21] Lin, C.-Y., Liu, J.-Y., Lin, C.-H., Sun, Y.-Y., Araujo-Pradere, E.A., Kakinami, Y.: Using the IRI, the MAGIC model, and the co-located ground-based GPS receivers to study ionospheric solar eclipse and storm signatures on July 22, 2009. *Earth, Planets and Space.* 64, 513-520(2012). <https://doi.org/10.5047/eps.2011.08.016>
- [22] Atıcı, R., Sağır, S., Emelyanov, L.Y., Lyashenko, M.: Investigation of Ionospheric Electron Density change during two partial Solar Eclipses and its comparison with predictions of NeQuick 2 and IRI-2016 models. *Wirel Pers Commun.* 118, 2239-2251 (2021). <https://doi.org/10.1007/s11277-021-08122-x>
- [23] Catherine, J.K., Uma Maheshwari, D., Gahalaut, V.K., Roy, P.N.S., Khan, P.K., Puviarasan, N.: Ionospheric disturbances triggered by the 25 April, 2015 M7.8 Gorkha earthquake, Nepal: Constraints from GPS TEC measurements. *J Asian Earth Sci.* 133, 80-88 (2017). <https://doi.org/10.1016/j.jseaes.2016.07.014>
- [24] Noll, C.E.: The crustal dynamics data information system: A resource to support scientific analysis using space geodesy. *Advances in Space Research.* 45, 1421-1440(2010). <https://doi.org/10.1016/j.asr.2010.01.018>
- [25] Seemala, G.K.: Estimation of ionospheric total electron content (TEC) from GNSS observations. In: *Atmospheric Remote Sensing*, pp. 63-84. Elsevier (2023)
- [26] KLOBUCHAR, J.A.: Ionospheric effect on GPS. *GPS World.* 2, 48-51(1991)
- [27] Nose, T. Iyemori, M. Sugiura, T. Kamei: World Data Center for Geomagnetism, Kyoto
- [28] Gonzalez, W.D., Joselyn, J.A., Kamide, Y., Kroehl, H.W., Rostoker, G., Tsurutani, B.T., Vasyliunas, V.M.: What is a geomagnetic storm? *J Geophys Res Space Phys.* 99, 5771-5792(1994). <https://doi.org/10.1029/93JA02867>

- [29] Zossi, B.S., Duran, T., Medina, F.D., de Haro Barbas, B.F., Melendi, Y., Elias, A.G.: Evaluating F2-region long-term trends using the International Reference Ionosphere(IRI)model: is this a feasible approximation for experimental trends? *Atmos Chem Phys.* 23, 13973-13986(2023). <https://doi.org/10.5194/acp-23-13973-2023>